High-Q plasmonic resonators based on metal split nanocylinders

G. Della Valle,[1,2] T. Søndergaard,[2] and S. I. Bozhevolnyi[2,3]
[1]*Dipartimento di Fisica and IFN-CNR, Politecnico di Milano, Piazza L. da Vinci 32, I-20133 Milan, Italy*
[2]*Department of Physics and Nanotechnology, Aalborg University, Skjernvej 4, DK-9220 Aalborg Øst, Denmark*
[3]*Institute of Sensors, Signals and Electrotechnics (SENSE), University of Southern Denmark, Niels Bohrs Allé 1, DK-5230 Odense M, Denmark*

(Received 2 July 2009; revised manuscript received 2 October 2009; published 3 December 2009)

In this paper we report on a detailed investigation of the quality Q factor exhibited by metal-nanostrip resonators with a bent axis. A detailed comparison of the Q with the quasistatic limit value demonstrates that under a large bending of the strip axis the resulting split-cylinder nanoresonators exhibit a Q that is exceeding the quasistatic Q in the near infrared. Also, a possible application of high-Q split-cylinder nanoresonators as high-sensitive plasmonic sensors is proposed.

DOI: 10.1103/PhysRevB.80.235405 PACS number(s): 73.20.Mf, 78.20.Bh, 42.25.−p, 71.36.+c

I. INTRODUCTION

In recent years, optical plasmon resonances[1] in metal nanostructures[2] have been extensively investigated because of their potential interest for challenging applications in nano-optics,[3,4] such as coherent control of light emission by single molecules,[5] new forms of local spectroscopy,[6] and coupling of classical radiation to single-quantum systems.[7] In this context, a design methodology allowing better control of the resonances is desirable to really address such applications,[4,8] with the resonance quality, i.e., its sharpness, becoming a key issue. Recently, the research interest has been focused on the development of plasmonic resonators based on slow surface-plasmon polaritons (S-SPPs) exhibiting wave-retardation effects (i.e., constructive interference of propagating back and forth S-SPP waves that are efficiently reflected by structure terminations).[9–13] Actually, S-SPP allows the electromagnetic field to be deeply squeezed in a subwavelength region, thus potentially leading to various ultrasmall (i.e., nanometer-sized)[14] resonators whose behavior can nevertheless be described only by incorporating the retardation effects. In particular, retardation results in a linear size-dependent tunability of the resonances in a broad wavelength range but also leads to a significant increase in the scattering loss, resulting in a radiation damping mechanism for the plasmon resonance. Therefore, the quality (Q) factor exhibited by S-SPP-based resonators is typically poor as compared to the Q of localized plasmon resonances observed in ultrasmall metal nanoparticles, which, under the quasistatic regime, is ultimately limited by ohmic losses in the metals.[15]

In a recent paper we proposed an innovative design for retardation-based plasmonic resonators allowing efficient suppression of radiation damping and thus resulting in a high-quality Q factor of the resonant structures approaching the quasistatic limit.[16] The underlying idea was to exploit the magnetic dipole response induced in a metal nanostrip after a conformal bending transformation.

In this paper we report on a more extensive investigation of the Q exhibited by bent nanostrips of different size in a broader wavelength range (spanning from 400 nm to 4 μm), aimed at a precise and quantitative comparison with the quasistatic value of Q.[15] Actually, the quasistatic Q, being ultimately limited by the ohmic losses in the metal, has been sometimes considered as the upper limit for the Q of any plasmonic resonator. Therefore, the possibility to achieve or eventually exceed this limit in S-SPP-based plasmonic structures exhibiting retardation effects is not only interesting from the theoretical point of view but, most importantly, plays a key role for the future development of efficient plasmonic nanoresonators for the real world.

II. QUALITY Q FACTOR: A DETAILED COMPARISON WITH THE QUASISTATIC Q

We considered thin silver strips of thickness t, having width w and different bending radii R surrounded by air (Fig. 1). The strip length along the z axis was assumed to be infinite, i.e., much longer than w, thus allowing a rigorous two-dimensional modeling in the xy plane based on the surface-integral equation method for the magnetic field.[17,18] Our previous analysis[16] revealed that the peak wavelength λ_P in the scattering spectrum exhibited under p-polarized plane-

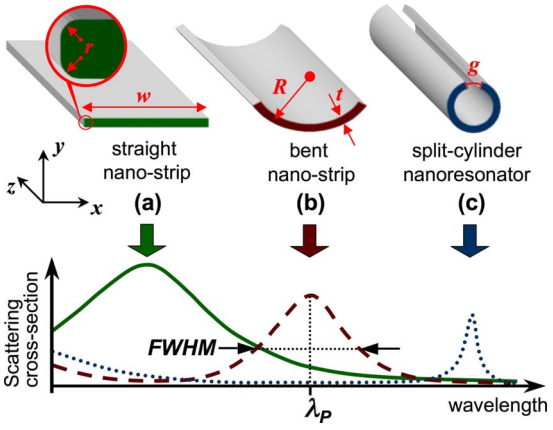

FIG. 1. (Color online) Schematic of the (a) straight, (b) bent, and (c) split-cylinder nanoresonators and qualitative scattering cross-section spectra exhibited under excitation with a p-polarized plane wave (i.e., electric field parallel to the x axis) propagating along y direction.

wave excitation is progressively redshifted and the Q factor (defined as the ratio between the resonance wavelength λ_P and the full width at half maximum of the scattering line) is progressively increased when the bending radius decreases (Fig. 1). In particular, numerical simulations based on silver refractive-index experimental data taken from Ref. 19 showed that under a strong bending of the structure the resulting split-cylinder nanoresonator exhibits a Q of the same order of magnitude as the quasistatic value Q_{st} given by the analytical formula derived by Wang and Shen,[15]

$$Q_{st} = -\frac{\lambda}{2\epsilon_m''}\frac{d\epsilon_m'}{d\lambda}, \tag{1}$$

where ϵ_m' and ϵ_m'' are the real and imaginary part of the silver relative dielectric constant ϵ_m and λ is the free-space wavelength. However, a quantitative comparison between Q_{st} and the Q exhibited by split-cylinder nanoresonators was prevented by the discrete nature of the experimental data employed for simulations, making any numerical computation of the derivative in Eq. (1) unreliable. Therefore, for a detailed analysis, we assume here a standard Drude-Sommerfeld analytical model (also accounting for one interband transition[20]) fitted on the refractive-index experimental data taken from Ref. 19.

In a first set of simulations we compared the Q_{st} with the numerically computed Q of the fundamental resonance exhibited in the scattering spectrum of silver nanostrips as the bending radius R is progressively decreased. Excitation with a p-polarized plane wave at an angle of 90° with respect to the x axis is assumed (Fig. 1). Two sets of nanostrips with different thicknesses and lengths are considered: $t=3$ nm and $w=50$ nm [Fig. 2(a)]; $t=20$ nm and $w=300$ nm [Fig. 2(b)]. Results of Fig. 2 reveal two distinct behavior of the Q depending on the size of the structures; for relatively small structures [Fig. 2(a)] as the bending radius decreases (and the bent nanostrip is turned into a split cylinder) the Q progressively approaches Q_{st}; on the contrary, for larger structures [Fig. 2(b)], the numerically computed Q, though being significantly lower than Q_{st} in the visible, first approaches and then becomes even higher than Q_{st} in the near infrared, before asymptotically converging to Q_{st}. Also, it is worth noting that as the bending radius is progressively decreased the resonance wavelength becomes more and more sensitive to small variations in R. We remind the reader to Sec. IV of the present paper for a detailed discussion of this particular behavior exhibited by split-cylinder nanoresonators.

In a second set of simulations we numerically computed the Q of the fundamental resonance in split-cylinder nanoresonators of a given thickness t and gap size g for increasing values of the strip width w. Actually, it has been reported that by acting on the parameter w the peak resonance wavelength in the scattering spectrum can be (almost linearly) tuned in a broad wavelength range from the optical to the infrared.[16] Four sets of structures with increasing size have been investigated, starting from $t=3$ nm, $g=1$ nm, and $r=1$ nm and scaling up the size of the structure by 3×, 6×, and 10×, respectively. The results are reported in Fig. 3 (triangles) aside with the quasistatic value Q_{st} (dotted line)

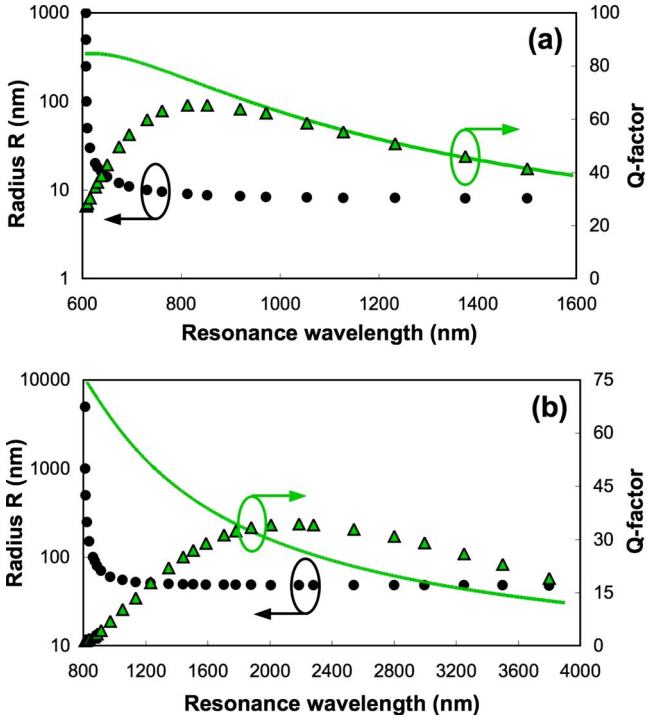

FIG. 2. (Color online) Bending radius R (circles) and Q factor (triangles) as a function of the resonance wavelength for two sets of silver bent nanostrips: (a) $t=3$ nm and $w=50$ nm; (b) $t=20$ nm and $w=300$ nm. The quasistatic quality factor Q_{st} from Eq. (1) is also reported (solid line).

and the (numerically computed) Q exhibited by straight nanostrips with $t=3$ nm and $r=1$ nm (circles) for comparison. Note that, in agreement with what reported in Fig. 2(a), the smallest split cylinders (for which $0.54\times10^{-2}<R/\lambda_P<1.1\times10^{-2}$) exhibit a Q that is almost coincident with the quasistatic value (rightward triangles in Fig. 3). However, as the structures are progressively scaled up, the resonance

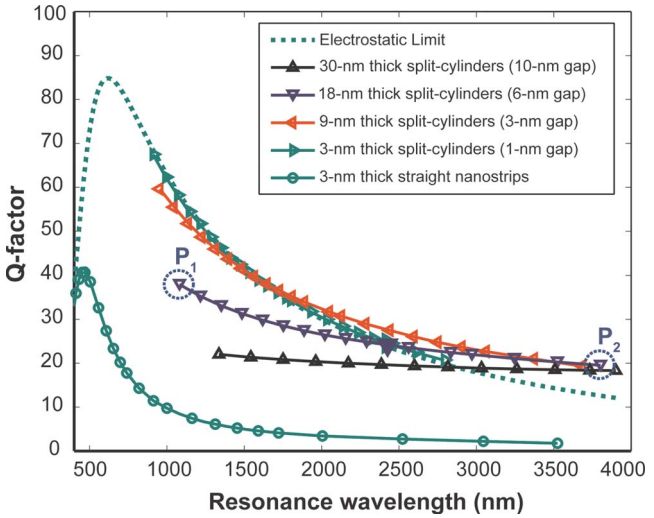

FIG. 3. (Color online) Dispersion of the Q for split-cylinder nanoresonators of different thickness and gap size (triangles). Results are compared to the Q of ultrathin straight nanostrips (circles) and to the quasistatic value, Q_{st} (dotted line).

wavelength is progressively redshifted. This circumstance indicates that though split-cylinder nanoresonators exhibit a Q as high as Q_{st}, they cannot be described according to a quasistatic approximation, that should predict a scale invariance for the plasmon resonance wavelength. Also, an even more unexpected feature is observed in the larger structures: while the Q deviates from Q_{st} toward lower values in the short-wavelength range, it becomes higher than Q_{st} for longer resonance wavelengths (i.e., longer strip widths), and the crossing between Q and Q_{st} is more and more redshifted as the strip width increases. This is a remarkably counterintuitive feature if we consider that the quasistatic Q_{st} given by Eq. (1) was derived assuming no radiation loss (only conduction, i.e., absorption loss was considered).[15] Though such approximation is certainly valid for ultrasmall nanostructures based on localized plasmon modes, exhibiting no retardation effects, for plasmonic structures based on propagating plasmon-polariton modes radiation loss cannot be disregarded and one could expect that the supplementary radiation damping should result in a Q significantly lower than Q_{st} at any wavelength. This is precisely what is observed for straight nanostrips (circles in Fig. 3) which have been demonstrated to behave like electric dipole scattering nanoantennas.[21] It is worth noting that the highest value of the ratio $Q/Q_{st} \sim 1.5$ is achieved in a split cylinder with 30 nm thickness, 10 nm gap, and 200 nm radius, which is a moderately large nanostructure. Though the relative increase in the Q as compared to Q_{st} is modest, this result demonstrates the feasibility of resonant nanostructures with high-quality factor as well as feasible size, which is an interesting feature not only from a theoretical point of view but also for real plasmonic applications.

III. EXPLANATION OF THE HIGH Q: THE CRUCIAL ROLE OF MAGNETIC ENERGY

In a recent paper[16] we showed that the radiation damping mechanism which is responsible for the low Q exhibited by straight nanostrips can be efficiently suppressed in bent nanostrips in view of a magnetic dipole response of the structure, thus becoming less radiating. Anyway, radiation losses cannot be completely suppressed, and the fact that Q can exceed the quasistatic limit remains counterintuitive unless we consider the following argument: in the quasistatic limit the energy stored in a plasmonic resonator is solely given by the electric field energy regardless the particular geometry of the structure;[15] on the contrary, in retardation-based plasmonic structures exhibiting a significant magnetic dipole response provided by a specially designed geometry, such as split-cylinder nanoresonators,[16] the localized magnetic field becomes an extra channel for energy storing which can strongly contribute to the Q. In order to check this argument we computed the electric field enhancement $|E/E_0|$ and the magnetic field enhancement $|H/H_0|$ (being E_0 and H_0 the complex electric and magnetic fields of the incident plane wave, respectively) in two different split cylinders of different size exhibiting the same resonance wavelength and a Q as high as Q_{st} (corresponding to the two almost overlapping solid triangles in Fig. 3). The results are reported in Fig. 4.

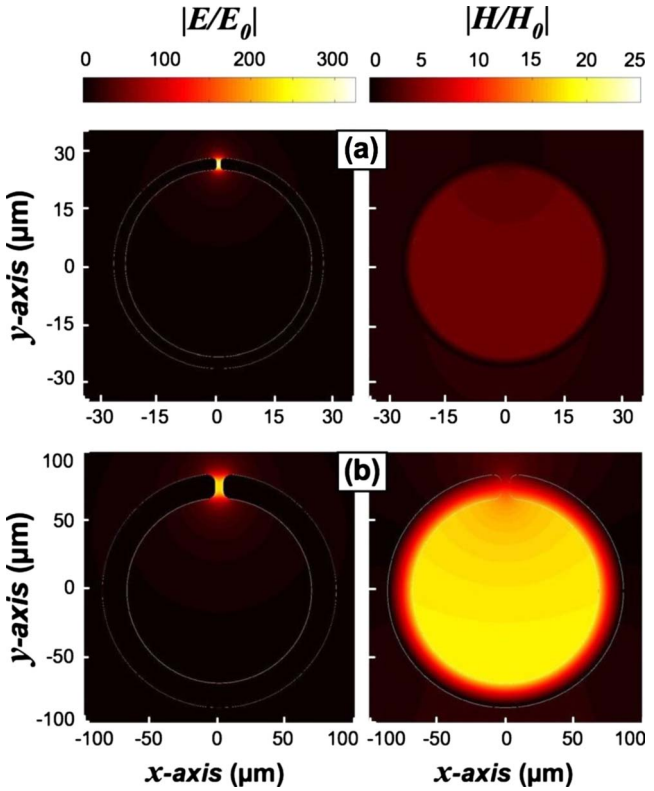

FIG. 4. (Color online) Resonant electric field enhancement (left panels) and magnetic field enhancement (right panels) in two different split-cylinder nanoresonators exhibiting the same resonance wavelength $\lambda_P = 2425$ nm and quality factor $Q = Q_{st} = 24.5$ at λ_P: (a) $t = 3$ nm, $R = 25.6$ nm, and $g = 1$ nm (solid rightward triangle in Fig. 3); (b) $t = 18$ nm, $R = 77.3$ nm, and $g = 6$ nm (solid downward triangle in Fig. 3).

Note that in the shortest structure [Fig. 4(a)] the magnetic field enhancement is relatively low (on the order of 4) as compared to the electric field enhancement which is as high as 300 in the gap region, (though a residual magnetic response is nevertheless exhibited). The high Q is thus ultimately due to the poor scattering cross-section peak (which is actually as low as 1.3 nm in this structure), resulting in very low radiation losses, (similarly to the case of ultrasmall structures under quasistatic regime, even if our structure exhibits retardation effects, as discussed in the previous section). On the contrary, in the largest structure, that exhibits a much higher scattering cross-section peak (of about 630 nm) and thus much higher radiation losses, the magnetic field enhancement also turns to be much higher (about 20) while the electric field enhancement is still as high as 300 [Fig. 4(b)]. Note that being the magnetic field localized in the whole area of the ring, the magnetic energy is expected to scale as the square of the cylinder radius R whereas the energy stored in the electric field is proportional to the circumference and thus scales linearly with the radius, being the electric field tightly bound to the metal as is in any plasmonic structure. Therefore, for a relatively large radius R it is expected that the radiation loss can be compensated with the storage of the magnetic energy. This situation is similar to that found when one considers the absorption and scattering

cross sections of nanospheres, that scale differently with the radius, causing the absorption becoming dominant for very small radii (and vice versa).

For a more quantitative evaluation of the role played by the magnetic field in the energy storing, we can compute the time-averaged electric and magnetic energy densities,[22]

$$\bar{w}_E = \frac{1}{4}\left[\epsilon' - \lambda\frac{d\epsilon'}{d\lambda}\right]_{\lambda_P}|E|^2, \tag{2}$$

$$\bar{w}_M = \frac{1}{4}\mu_0|H|^2, \tag{3}$$

where ϵ' is the real part of the dielectric constant in the dielectric or in the metal (i.e., $\epsilon' = \epsilon_d$ in the dielectric and $\epsilon' = \epsilon'_m$ in the metal). The electric energy $\mathcal{E}_E$ and the magnetic energy $\mathcal{E}_M$ stored in the structure can thus be estimated by integrating Eqs. (2) and (3), respectively, over an area in the xy plane comprising the scattered near field of the structure. Remembering that for the incident plane wave we have $E_0 = -i\sqrt{\mu_0/(\epsilon_0\epsilon_d)}H_0$, the ratio $\Gamma = \mathcal{E}_M/\mathcal{E}_E$ can be finally estimated and turned to be $\Gamma \simeq 4.5\%$ in the split cylinder with the smallest area and $\Gamma \simeq 43\%$ in the split cylinder with the largest area. A similar behavior is observed if we compare two different split cylinders of the same thickness and gap size and different ring lengths, e.g., $t=18$ nm, $g=6$ nm and $w_1=180$ nm and $w_2=780$ nm, respectively, which are represented by points P_1 and P_2 in Fig. 3. Note that the first structure exhibits a Q which is significantly lower than Q_{st} at the corresponding resonance wavelength ($\lambda_{P1}=1082$ nm) and the Γ ratio turns to be $\Gamma_1=12\%$. On the contrary, the second (largest) structure exhibits a Q exceeding Q_{st} at the corresponding resonance wavelength ($\lambda_{P2}=3802$ nm) and the Γ ratio turns to be $\Gamma_2=56\%$. Nevertheless it is worth noting that the Q decreases in absolute value as the radius of the split cylinder increases (and thus the resonance wavelength is correspondingly redshifted; see Fig. 3) but the rate of decrease is lower than that of Q_{st} and this causes the Q to significantly exceed Q_{st} in the long-wavelength range for moderately large structures. These results indicate that the magnetic energy becomes an efficient channel for energy storing as (for a given gap width) the radius of the split cylinder increases and can thus strongly contribute to the Q and eventually cause the quality factor to exceed the quasistatic value Q_{st} at the corresponding wavelength.

Finally, note that the Q can be estimated also according to a different though equivalent approach, namely, by computing the stored energy as a function of the excitation wavelength. In fact, this approach offers the possibility to separate the two different contributions provided to the Q by the electric energy and by the magnetic energy stored in the near field of the nanostructure. As example, in Figs. 5(a) and 5(b) we report the electric stored energy and the magnetic stored energy, respectively, as a function of the excitation wavelength for the two different split cylinders represented by points P_1 and P_2 of Fig. 3. Note that despite of the different values of the Q exhibited by the two structures (respectively, below and above Q_{st}) for each structure the electric and the magnetic energy exhibit the same resonance wavelength as well as the same resonance width. The same behavior was observed in all the structured we examined, in agreement with the fundamental fact that the electric and the magnetic fields are coupled together by Maxwell's equations, and thus are expected to follow the same decay rate. This is also an indication that the electric dipole mode and the magnetic dipole mode sustained by a split-cylinder resonator are coupled together, i.e., the fundamental resonant mode of a split-cylinder resonator is an hybridized mode originating from an electric dipole mode and a magnetic dipole mode; in the short-wavelength range or for very small structures it is the electric mode that dominates (and thus stores most of the energy); on the contrary, in the long-wavelength range and for moderately large structures a significant amount of energy is also stored in the magnetic part of the mode.

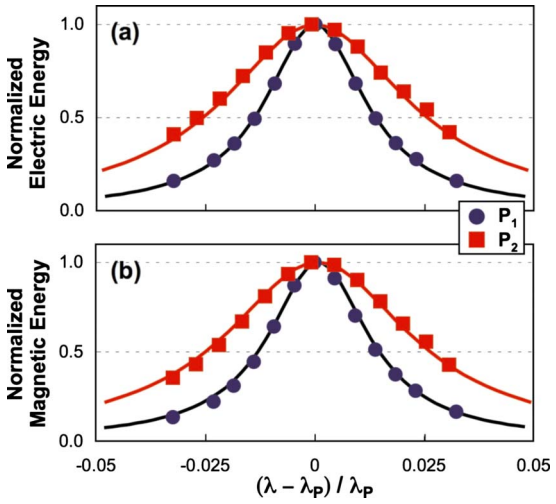

FIG. 5. (Color online) Normalized (a) electric and (b) magnetic energies stored in the two split-cylinder resonators corresponding to points P_1 (squares) and P_2 (circles) of Fig. 3 as a function of the (normalized) detuned excitation wavelength. Solid lines: Lorentzian fitting curves with quality factor of 36 and 19 for P_1 and P_2, respectively, in excellent agreement with the Q estimated from the scattering cross-section resonance linewidths (Fig. 3).

IV. HIGH Q FOR SENSING APPLICATIONS

The analysis above reported demonstrates that moderately large split-cylinder nanoresonators can exhibit a high-quality factor, indeed as high as the Q_{st} or even higher in the near infrared. This feature, together with the linear size-dependent tunability and the high field enhancement demonstrated in a broad wavelength range,[16] makes split-cylinder nanoresonators very attractive for sensing applications. It is worth noting that, contrary to ultrasmall plasmonic nanostructures where the smallest radius of curvature is the most critical parameter (leading to large variations in the observed resonant behavior for nominally identical structures), split-cylinder nanoresonators are intrinsically robust, being the resonance wavelength, the quality factor and the field enhancement weakly sensitive to the local radius of curvature r at strip terminations.

More precisely, Fig. 6 demonstrates that after 300% variation in r only a few percent variation in the resonance wave-

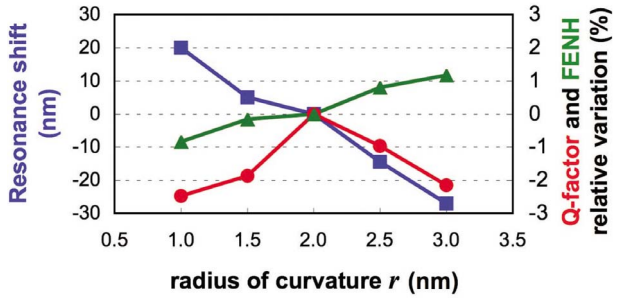

FIG. 6. (Color online) Resonance wavelength (squares), Q factor (circles), and field-enhancement (triangles) sensitivity to the variations in the nanometer-sized radius of curvature r at strip terminations for a split-cylinder nanoresonator of 300 nm width, 20 nm thickness, and 5 nm gap (resonance wavelength at 1818 nm for $r=2$ nm).

length, Q factor, and field enhancement is expected in a 300-nm-wide, 20-nm-thick, and 5-nm-gap split-cylinder nanoresonator. Actually, the most sensitive parameter of the structure turns to be the gap size g, as can be easily revealed if we redraw the data of Fig. 2 by plotting the resonance wavelength as a function of g instead of R (Fig. 7). Note that under few nm variation in the gap size, the resonance wavelength experiences very large variations. Rather than being a limitation, this behavior, combined with the high Q of the structure, can be profitably exploited to make a sensing device out of a single split-cylinder nanoresonator. Actually, if the structure was compressed or stretched along the x axis, its deformation (and the strength of the compressing or stretching force after proper calibration) could be accurately recovered by inspecting the large-wavelength shift in the resonant peak of the scattering cross section. As example, at 1.55 μm (i.e., at the telecom) resonance wavelength $d\lambda/dg \simeq 50$ (Fig. 7) and the Q is as high as 30 (Fig. 2). Therefore, a resonance shift of few nanometers corresponds to a gap deformation of about 1 Å, and a single split-cylinder nanoresonator, coupled to a high-sensitive photodetector (i.e., a single-photon avalanche photodiode) can provide, in principle, an effective optomechanical transducer with atomic resolution.[14]

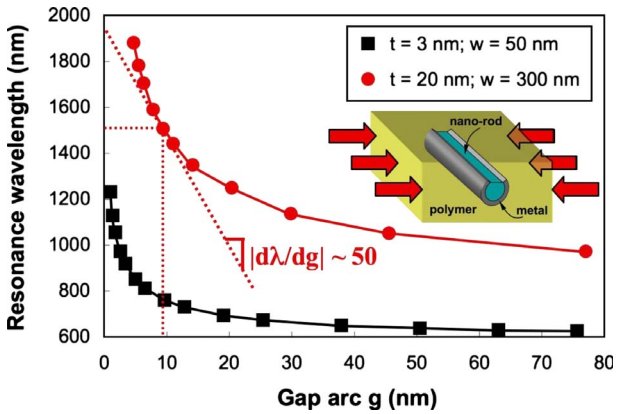

FIG. 7. (Color online) Resonance wavelength as a function of the gap arc g for the bent nanostrips of Fig. 2. Inset shows a sketch of a possible realization of the split-cylinder nanosensor based on a nanorod schaphoid and a polymer as a surrounding medium.

As a note on feasibility, we believe that split-cylinder nanoresonators could be fabricated in a double step process; in a first step, a closed-cylinder structure is produced by using a single dielectric nanorod as a schaphoid for thin metal film deposition; then, the ring splitting can be obtained by ion-beam milling. The final structure should be embedded in a polymer possibly matching the refractive index of the nanorod material, and a split-cylinder nanosensor should appear as sketched in the inset of Fig. 7. Further numerical analysis of such a composite (three-media) structure is required in order to quantitatively account for the residual asymmetry of the dielectric environment surrounding the nanostrip. Nevertheless, it is well known that a slow (and short range) SPP mode with no cutoff always exist in an asymmetric insulator-metal-insulator structure,[23] and thus the unique features exhibited by split-cylinder nanoresonators embedded in a uniform dielectric are expected to be substantially preserved in the case of slight asymmetries of the surrounding medium. Another issue to be considered for real sensing applications is that the application of a pointlike or, more generally, of a stretching or compressing force which is nonuniform along z direction would result in a nonuniform distortion of the gap, causing anomalous response of the split-cylinder nanosensor or degradation of its effective sensitivity. To reduce these detrimental effects the length of the split cylinder would be limited to few micron (at the expense of a lower signal-to-noise ratio in the detected scattered radiation) making the structure more rigid along z direction, and thus less sensitive to nonuniform deformations.

V. CONCLUSION

In conclusion, we reported on a detailed numerical analysis of the quality factor exhibited by the fundamental scattering resonance of split-cylinder nanoresonators. Our simulations considered several structures of different size and a broad range of excitation wavelengths, from the visible to the near infrared. We found that under a strong bending of structures, split-cylinder nanoresonators exhibit a Q that exceeds the quasistatic limit in the long-wavelength range even in a moderately large structure and yet with complete retardation effects. A detailed computation of the energy stored in the near field of the structures revealed that this counterintuitive feature can be explained in terms of the extra channel for energy storing provided by magnetic field excitation. Actually, the quasistatic regime is characterized by the dominance of the electric field and absorption leading to a limit in Q. Using slow plasmon-modes retardation introduces the increase in the scattering loss, which results in a poor Q for structures with a simple linear geometry, such as straight nanostrips. Anyway, contrary to the case of the quasistatic limit, where geometry plays no role, retardation effects gives the possibility to create resonant magnetic fields (forming magnetic dipoles for the fundamental resonances) under a proper design of the geometry, as we know from gap resonators[24] and split-cylinder resonators.[16] The overall effect on Q thus depends on the balance between these two new contributions, and this is the transition we carefully explored in this paper. In particular, split-cylinder resonators

turned to be more effective in achieving this compensation, as compared to gap resonators, in view of a higher degree of freedom. Actually, here we have two knobs: the radius and the gap. The radius gives the possibility to increase the relative ratio of the magnetic energy stored at resonance (as discussed above) and the gap gives the possibility to suppress the scattering loss.

Therefore, depending on the geometry of the structure, retardation effects can enhance the Q instead of decreasing it. This result is in line with what has been recently reported in another theoretical investigation[25] where the authors demonstrated that, in view of retardation effects, a deep-subwavelength resonant mode exists in ultrasmall three-dimensional plasmonic resonators allowing a Q factor exceeding Q_{st}.

Also, another interesting feature exhibited by split-cylinder nanoresonators has been put in evidence, namely, the strong sensitivity of their plasmonic resonance to the gap size of the split cylinder. This feature, aside with the high Q, makes split-cylinder nanoresonators potentially suitable for sensing at the nanoscale, and an optomechanical transducer for deformation detection with atomic resolution has been proposed.

ACKNOWLEDGMENT

G. Della Valle gratefully acknowledges financial support from the Fondazione Silvio Tronchetti Provera.

[1] H. Räther, *Surface Plasmons* (Springer, New York, 1988).
[2] M. Pelton, J. Aizpurua, and G. Bryant, Laser Photonics Rev. **2**, 136 (2008).
[3] P. Mühlschlegel, H.-J. Eisler, O. J. F. Martin, B. Hecht, and D. W. Pohl, Science **308**, 1607 (2005); J.-J. Greffet, *ibid.* **308**, 1561 (2005).
[4] M. F. Garcia-Parajo, Nat. Photonics **2**, 201 (2008).
[5] S. Kühn, U. Håkanson, L. Rogobete, and V. Sandoghdar, Phys. Rev. Lett. **97**, 017402 (2006).
[6] T. Kalkbrenner, U. Håkanson, A. Schädle, S. Burger, C. Henkel, and V. Sandoghdar, Phys. Rev. Lett. **95**, 200801 (2005).
[7] J. N. Farahani, D. W. Pohl, H.-J. Eisler, and B. Hecht, Phys. Rev. Lett. **95**, 017402 (2005).
[8] A. Alù and N. Engheta, Nat. Photonics **2**, 307 (2008).
[9] S. A. Maier, Opt. Quantum Electron. **38**, 257 (2006).
[10] H. T. Miyazaki and Y. Kurokawa, Phys. Rev. Lett. **96**, 097401 (2006).
[11] Y. Kurokawa and H. T. Miyazaki, Phys. Rev. B **75**, 035411 (2007).
[12] T. Søndergaard and S. Bozhevolnyi, Phys. Rev. B **75**, 073402 (2007).
[13] E. Feigenbaum and M. Orenstein, Opt. Express **15**, 2607 (2007).
[14] Hereafter we implicitly assume that the decrease in structure dimensions is limited only by the limit of validity of the concept of macroscopic dielectric constant that becomes questionable for few-atom structures.
[15] F. Wang and Y. R. Shen, Phys. Rev. Lett. **97**, 206806 (2006).
[16] G. Della Valle, T. Søndergaard, and S. I. Bozhevolnyi, Phys. Rev. B **79**, 113410 (2009).
[17] T. Søndergaard, Phys. Status Solidi B **244**, 3448 (2007).
[18] J. Jin, *The Finite Element Method in Electromagnetics*, 2nd ed. (John Wiley & Sons, New York, 2002).
[19] P. B. Johnson and R. W. Christy, Phys. Rev. B **6**, 4370 (1972).
[20] L. Novotny and B. Hecht, *Principles of Nano-Optics* (Cambridge University Press, Cambridge, 2006).
[21] T. Søndergaard and S. I. Bozhevolnyi, Opt. Express **15**, 4198 (2007).
[22] E. J. Rothwell and M. J. Cloud, *Electrodynamics* (CRC, London, 2001).
[23] J. J. Burke, G. I. Stegeman, and T. Tamir, Phys. Rev. B **33**, 5186 (1986).
[24] S. I. Bozhevolnyi and T. Søndergaard, Opt. Express **15**, 10869 (2007).
[25] E. Feigenbaum and M. Orenstein, Phys. Rev. Lett. **101**, 163902 (2008).